ELSEVIER

Journal of Nuclear Materials 301 (2002) 64–69

journal of nuclear materials

www.elsevier.com/locate/jnucmat

# Atomistic simulation of liquid lead and lead–bismuth eutectic

Massimo Celino [a,b], Roberto Conversano [a], Vittorio Rosato [a,b,*]

[a] *Ente per le Nuove Tecnologie, l'Energia e l'Ambiente (ENEA), Centro Ricerche Casaccia, HPCN Project, P.O. Box 2400, I-00100 Roma, Italy*

[b] *Istituto Nazionale di Fisica della Materia (INFM), Unitá di Ricerca Roma 1, Italy*

**Abstract**

Lead and the Pb–Bi eutectic (Pb 55.9 at.%) have been modeled by a *n*-body potential derived from a second moment approximation of a tight binding Hamiltonian. The thermal behavior of the two systems in the liquid phase has been reproduced and relevant structural parameters have been evaluated and compared with experimental data. The diffusion coefficients and the activation energy for diffusion have been also evaluated. 

*PACS:* 61.20.Ja; 61.25.Mv; 65.20.+w; 72.15.Cz

## 1. Introduction

Liquid lead and the Pb–Bi eutectic (LBE hereafter, is a metallic alloy of composition Pb 55.9 at.% stable in the liquid phase) constitute a similar option for the use as coolant systems for the primary circuit of special-purpose nuclear power installations. The design of future sub-critical reactors of the ADS family [1] envisages the use of liquid Pb or LBE as both coolant and spallation target for neutron amplification. Therefore, several european programs (TECLA [2], MEGAPIE [3], SPIRE [4]) are going to collect data on both the chemical and the physical properties of these materials. A particular interest is devoted to the understanding of the corrosion phenomena engendered by Pb and LBE, at the working thermodynamic conditions, when in contact with the materials composing the containing pipes of the vessel.

The most relevant property of both Pb and LBE is the large gap between the melting $T_M$ and the boiling $T_B$ temperatures ($T_M = 601$ K and $T_B = 2022$ K for Pb, $T_M = 396$ K and $T_B = 1943$ K for LBE); this property enhances the reliability and the safety of the installation. The high density ($\rho = 10.33\ \mathrm{g\,cm^3}$ at $T = 873$ K for Pb, $\rho = 10.242\ \mathrm{g\,cm^3}$ at $T = 673$ K for LBE) and a large heat capacity ($C_p^{(\mathrm{exp})} = 150\ \mathrm{J\,kg^{-1}\,K^{-1}}$ at $T = 873$ K for Pb, $C_p^{(\mathrm{exp})} = 146\ \mathrm{J\,kg^{-1}\,K^{-1}}$ at $T = 673$ K for LBE), are further properties which enforce the attitude of these systems for the envisaged applications.

This work attempts to apply an atomic-scale model, developed for transition metals and alloys [5,6], to Pb and LBE, in order to evaluate the most relevant structural and dynamical quantities. The resulting models will then be used, in future works, to the study of the microscopic-scale processes at the origin of phenomena such as liquid metal embrittlement (LME) and corrosion. The mutual solubility of the host and the embrittler, for instance, has been thought as a necessary pre-requisite for producing wetting (and, thus, for inducing corrosion) and for triggering interdiffusion in the host (and, hence, for being responsible of embrittlement). These views have been recently criticized [7] as it has been shown that also very low solubility can produce sizeable corrosion and embrittlement phenomena. In this respect, reliable microscopic-scale models, able to reproduce the behavior of the interacting species, could be extremely useful for a deeper understanding of these phenomena.

In this work we perform a number of molecular dynamics simulations, at finite temperatures, to predict

* Corresponding author. Tel.: +39-6 3048 4825; fax: +39-6 3048 4729.

*E-mail address:* rosato@casaccia.enea.it (V. Rosato).

0022-3115/02/$ - see front matter 
PII: S0022-3115(01)00729-2

thermodynamic, structural and transport properties to complement the body of data which is going to be assembled on these systems.

## 2. Computational method

The atomic interaction of Pb and Bi have been modeled by using a $n$-body interaction scheme, resulting from a second moment approximation of a tight binding Hamiltonian [5,6]. In this scheme, the potential energy $U$ of the system is described by

$$U = \sum_{i=1}^{N}\sum_{j=1}^{N} A_{\alpha,\beta}\exp[-p_{\alpha,\beta}(r_{ij}/r^0_{\alpha,\beta}-1)] - \sum_{i=1}^{N}\left\{\sum_{j=1}^{N}\xi^2_{\alpha,\beta}\exp[-2q_{\alpha,\beta}(r_{ij}/r^0_{\alpha,\beta}-1)]\right\}^{1/2}, \quad (1)$$

where $A_{\alpha,\beta}$, $\xi_{\alpha,\beta}$, $p_{\alpha,\beta}$, $q_{\alpha,\beta}$ and $r^0_{\alpha,\beta}$ are suitable parameters which depend on the atomic species $\alpha$ and $\beta$ of the interacting particles $i$ and $j$. These parameters are fitted, for the pure species, on properties such as the potential energy and the elastic constants and by imposing a vanishing pressure at the equilibrium lattice spacing. For the cross-terms, in absence (as in this case) of any intermetallic alloy with the composition close to that of the LBE (this would have enabled the same type of parameters fitting as that used for pure systems), we have used only the enthalpy of mixing of the two species and the equilibrium density at a given temperature. The Pb parameters are those originally evaluated by Ref. [6]. For the definition of the LBE model, we have firstly evaluated the pure Bi parameters (experimental data taken from Ref. [8]). Then we have guessed a first set of the cross-interactions parameters by taking the geometrical average of the corresponding pure systems parameters. A LBE liquid system has been thus produced with $N = 1000$ atoms ($N_{Pb} = 559$, $N_{Bi} = 441$) contained in a computational box whose volume is such to produce a system density of 0.030163 Å$^{-3}$ (equal to the experimental density value at $T = 600$ K [9]). Keeping the volume fixed, we heated up the system at $T = 1000$ K and then we slowly cooled it down to $T = 600$ K. At this temperature, we perform a variation of the cross-terms parameters of the potential in order to obtain: (1) a vanishing pressure for the considered volume and (2) a potential energy equal to

$$U = \alpha U_{Pb} + (1-\alpha)U_{Bi} - \Delta H_{mix}, \quad (2)$$

where $\alpha$ is the atomic fraction of Pb and $\Delta H_{mix} = 0.011$ eV is the mixing enthalpy of the two species at the considered stoichiometry, as resulting from the available thermodynamic data at $T = 700$ K [10]. The length scale of the mixed interaction $r^0_{Pb,Bi}$, moreover, has been determined by allowing the radial distribution function of the LBE liquid, at 600 K, to be as close as possible with the experimental data [11]. This task has been accomplished by using the so-called reverse Monte Carlo (RMC) method [12,13]; the experimental radial distribution function of the LBE system [11] has been used as a target function to be reproduced by the atomic-scale structure of the liquid. The positions of the atoms in the computational box were randomly displaced and the moves accepted or rejected as a function of the resulting 'distance' between the calculated and the experimental radial distribution functions (with the usual Boltzmann condition at a given fictitious temperature). After the RMC procedure, the potential parameters have been re-adjusted to ensure the fulfillment of the points (1) and (2) stated above. The potential parameters resulting from this complex adjustment procedure are reported in Table 1.

Table 1
Potential parameters for the LBE system

| | $A$ (eV) | $\xi$ (eV) | $p$ | $q$ | $r^0$ (Å) |
|---|---|---|---|---|---|
| Pb–Pb | 0.09800 | 0.9140 | 9.5760 | 3.6480 | 3.500 |
| Bi–Bi | 0.07189 | 0.8730 | 10.7065 | 2.8239 | 3.687 |
| Pb–Bi | 0.06500 | 0.8490 | 10.0000 | 3.2000 | 3.400 |

## 3. Results

### 3.1. Lead

For the pure Pb, a system containing $N = 500$ atoms has been used. The system was simulated at different temperatures, from $T = 150$ up to $T = 900$ K, in a large temperature domain. This allows one to evaluate different thermodynamic quantities used to check the model accuracy versus experimental data. In Fig. 1 we report the behavior of the potential energy and the volume as a function of temperature. From this figure, it is possible to evaluate both the heat capacity and the linear expansion coefficient; the first results to be $C_p = 16.8$ J mol$^{-1}$ K$^{-1}$ ($C_p^{(exp)} = 26.4$ J mol$^{-1}$ K$^{-1}$) at $T = 300$ K; the second, evaluated at the same temperature, $\alpha_V = 5.6 \times 10^{-5}$ K$^{-1}$ ($\alpha_V^{(exp)} = 2.9 \times 10^{-5}$ K$^{-1}$ [8]). Thermodynamic data allow one to locate the melting temperature of the model at $T_M \sim 610$ K, the latent heat at melting $\Delta H = 0.05$ eV/atom ($\Delta H(exp) = 0.049$ eV/atom [8]) and a latent volume at melting $\Delta V = 2.174$ Å$^3$/atom. Fig. 2 reports the radial distribution function $g(r)$ of pure of lead at $T = 300$ K (left panel) and $T = 700$ K (right panel). In the latter panel, we also report the experimental radial distribution function of liquid lead [11].

The dynamical trajectories of the particles allowed the self-diffusion coefficient to be evaluated. The calculated

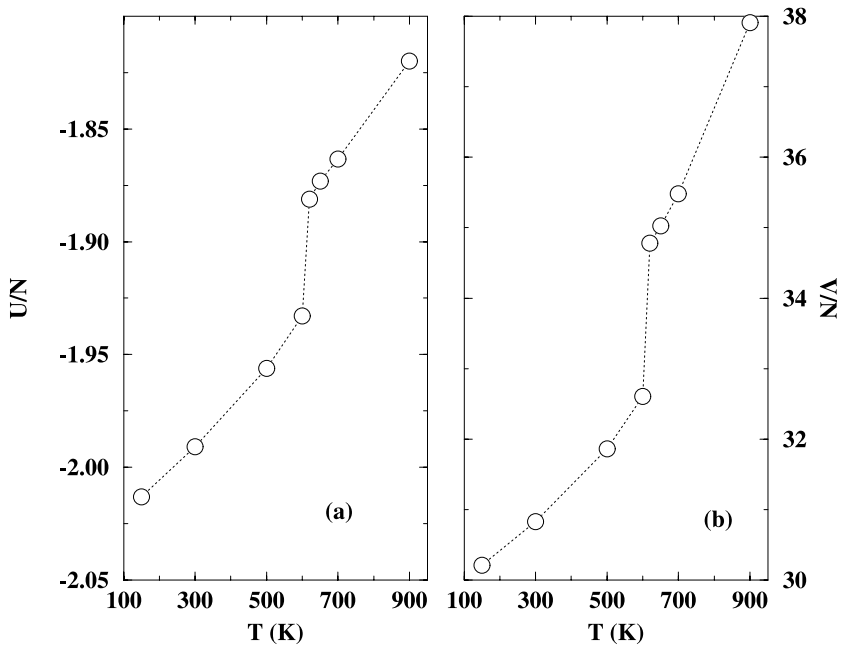


Fig. 1. Thermal behavior of the potential energy (left) and the volume (right) per atom, for the pure Pb system. Potential energy $U/N$ in eV/atom; atomic volume $V/N$ in $\text{Å}^3$.

values are: $D\ (T = 700\ \text{K}) = 2.8 \times 10^{-5}\ \text{cm}^2/\text{s}$ and $D\ (T = 900\ \text{K}) = 5.3 \times 10^{-5}\ \text{cm}^2/\text{s}$. The resulting activation energy for diffusion $E_\text{A}$ is thus $E_\text{A} = 0.17$ eV.

### 3.2. LBE

The system was left free to reach a thermodynamic equilibrium at different temperatures, in the range of existence of the liquid phase, from $T = 500$ to 800 K. The evaluation of the equilibrium volumes at the different temperatures allows to estimate the volume expansion coefficient $\alpha_V$ which results to be $\alpha_V = 1.32 \times 10^{-4}\ \text{K}^{-1}$ ($\alpha_V^{(\text{exp})} = 1.2 \times 10^{-4}\ \text{K}^{-1}$ [9]). The heat capacity $C_p$ was also evaluated, from the potential energy data; it results to be $C_p = 80\ \text{J}\,\text{Kg}^{-1}\,\text{K}^{-1}$ whereas the experimental value is $C_p^{(\text{exp})} = 146\ \text{J}\,\text{Kg}^{-1}\,\text{K}^{-1}$ for LBE [9].

A further relevant information on the LBE system can be achieved by evaluating the total radial distribution function $g(r)$ and its partial components $g_{\text{Pb Pb}}(r)$, $g_{\text{Bi Bi}}(r)$ and $g_{\text{Pb Bi}}(r)$ (Fig. 3 reports the evaluated functions). The position of the first peak of the total radial distribution function $r_1$, evaluated on the model system is $r_1 = 3.22$ Å in agreement with neutron diffraction studies [11] indicating $r_1 = 3.25$ Å. In particular, the strongest signal comes from the $g_{\text{Pb Bi}}(r)$ which has a sharp maximum at $r_1 = 3.12$ Å. The model system seems to be unable to reproduce the shoulder (which is clearly visible at $4.6 \leqslant r \leqslant 5.4$ Å in the radial distribution function taken from neutron diffraction data [11]). This feature, probably determined by a secondary structure of the pure Bi radial distribution function, seems to be reminiscent of the parent crystalline structure which, in its R3m structure, has neighbors peaks at $r = 4.74$ and 5.55 Å (third and fourth neighbors, respectively). This could suggest the presence in the experimental sample of regions with large compositional dishomogeneity.

We have firstly integrated the total radial distribution function up to its first minimum ($r = 4.6$ Å) to predict the average first neighbors coordination $Z$ which turns out to be $Z = 12.5$; the integration of the experimental curve up to the same distance provides a coordination value $Z(\text{exp}) = 12.2$. The slight disagreement would probably arise from the rough approximation that the model system provides of the region between the first and the second neighbors. We have also integrated the partial radial distribution functions up to the position of the first minimum of the total $g(r)$, in order to find particle's coordination $Z_i$. In Table 2, other than the total coordination of the single species, we also report the values of $z_{ij}$, the average number of species $j$ surrounding species $i$ within the first coordination shell. The knowledge of $z_{ij}$ allows the chemical short range order (CSRO) parameters $\alpha_{ij}$ [14] to be defined:

$$\alpha_{ij} = 1 - z_{ij}/c_j Z_i, \tag{3}$$

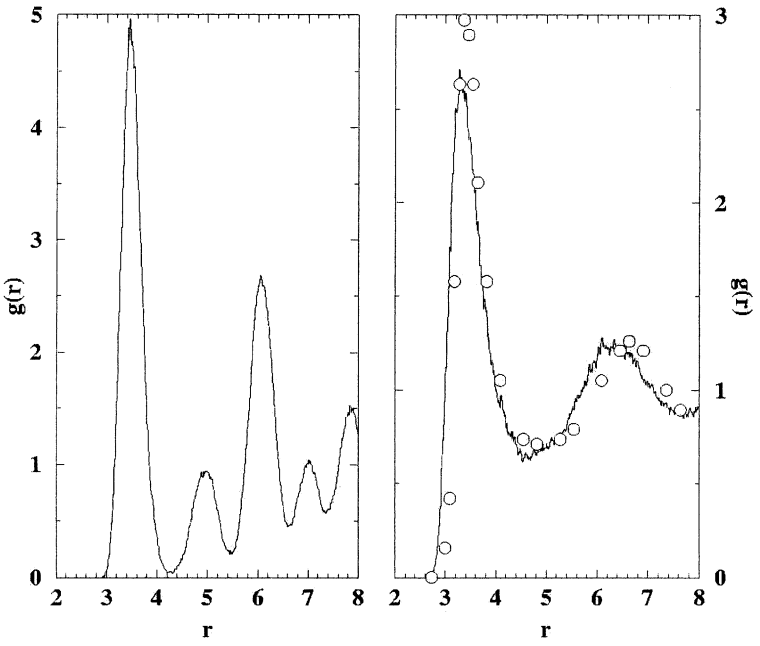


Fig. 2. Radial distribution functions of the Pb system at different temperatures: $T = 300$ K (left panel); $T = 700$ K (right panel). In the latter panel, the experimental radial distribution function $g(r)$ of pure Pb, taken from Ref. [11], is also reported (○). Distances $r$ in Å.

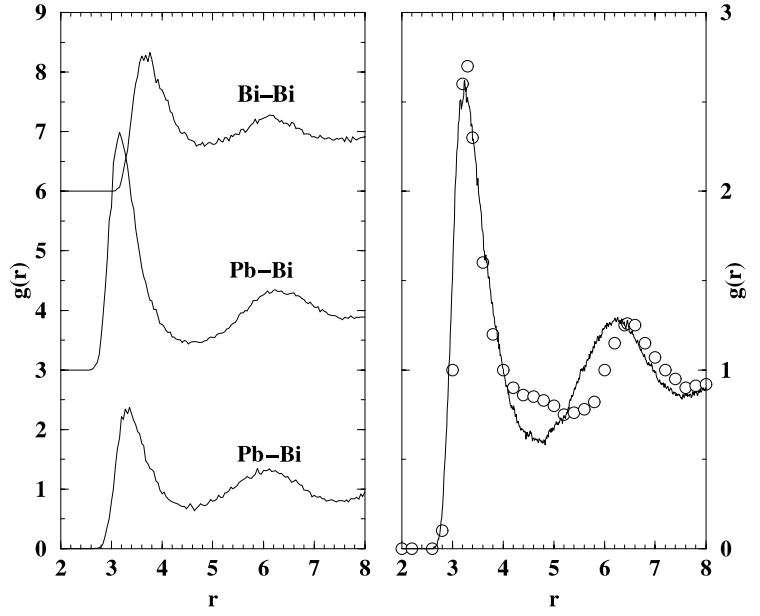


Fig. 3. Radial distribution functions of the LBE system at $T = 600$ K. Left panel: the different partial distribution functions of the different species; right panel: total radial distribution function (—) and experimental data (○) taken from Ref. [11]. Distances $r$ in Å.

where $c_j$ is the concentration of species $j$ and $Z_i = z_{ii} + z_{ij}$, the total coordination number around species $i$. The negative values of $\alpha$ factors for the mixed Pb–Bi couples indicate a preference for unlike neighbor bonds. Moreover, the fact that $\alpha_{\mathrm{Pb\,Bi}} < \alpha_{\mathrm{Bi\,Pb}}$ indicates that the degree of CSRO is enhanced around Pb atoms relative to Bi atoms.

The mean-square displacements $r^2(t)$ of the atoms of the two species have been evaluated at $T = 600$ and 800 K. The absolute values of the diffusion coefficients of the

Table 2
Average coordinations and CSRO parameters $\alpha_{ij}$ for the different couples at $T = 600$ K ($T = 800$ K)

| | $z_{ij}$ | $c_j$ | $Z_i$ | $\alpha_{ij}$ |
|---|---|---|---|---|
| Pb–Pb | 6.43 (6.40) | 0.559 | 14.3 (14.2) | 0.19 (0.19) |
| Pb–Bi | 7.85 (7.80) | 0.441 | 14.3 (14.2) | −0.25 (−0.25) |
| Bi–Bi | 5.32 (5.29) | 0.441 | 11.5 (11.4) | 0.03 (0.04) |
| Bi–Pb | 6.20 (6.15) | 0.559 | 11.5 (11.4) | −0.05 (−0.05) |

two species evaluated at $T = 600$ K are: $D$ (Pb) = $1.4 \times 10^{-5}$ and $D$ (Bi) = $1.2 \times 10^{-5}$ cm$^2$/s. The average slope of the values of the diffusion coefficients has provided an estimate of the activation energy for diffusion $E_A$, which results to be $E_A$ (Pb) = 0.1 eV and $E_A$ (Bi) = 0.08 eV.

## 4. Conclusions

Reliable atomic-scale models of Pb and the LBE system have been derived from a $n$-body interatomic potential. This scheme, although being affected by a number of physical approximations, has proven to reproduce, with a reasonable accuracy, the essential features of the metallic bonding. The model has been devised, however, to reproduce the system in the liquid phase (e.g. $T \geqslant 400$ K), as any intermetallic or solid solutions is predicted to occur, at equilibrium, for the considered Pb–Bi stoichiometry. The model predictions have been compared with the available structural information (i.e. the radial distribution function of the eutectic) and with some thermodynamic data (the volume expansion coefficient, the heat capacity). In both cases the agreement between predictions and experimental data is quite satisfactory; this fact authorizes one to be confident on the predictions which can be made from the model analysis.

The model systems will now be used to describe the liquid Pb and the LBE interaction with metallic surfaces, with the aim of understanding the atomic-scale mechanisms of the corrosion phenomena and of LME [7]. This will hopefully provide a relevant body of data to be used in the technological design of the materials which will be used in the TECLA project [2]. Future works will be devoted to the definition of further model potentials to reproduce interactions between Pb, LBE and an iron surface. This will be done by deriving an empirical scheme from a first-principles model [15]. It is well known, in fact, that both lead and bismuth have a vanishingly small solubility in iron [10]. The absence of any data on the form and the strength of the interaction among these species will compel the use of first-principles calculations to predict the shape and the value of a distance-dependent interaction potential which will be cast in a functional form like that of Eq. (1). This interaction model, in conjunction with that developed in this work for the LBE system, will allow several *gedanken* experiments to be performed which should allow to answer to questions such as: (1) is the stress–strain behavior of the solid metal influenced by the presence of the LBE before the fracture occurs? (2) is the dislocation nucleation at the crack-tip enhanced by the adsorption of liquid metal atoms? (3) which is the extent of the bond weakening due to the lowering of the surface energy at the crack tip? (4) which mechanism initiates the crack when embrittlers penetrate into GB's and lower the crack resistance?

The answer to these questions will be of invaluable help in technological studies as they will contribute to the understanding of phenomena occurring in materials under severe thermodynamic and chemical conditions as those met in nuclear devices.

## Acknowledgements

The work has been supported by the UE Project TECLA (Technologies, materials and thermal-hydraulics for Lead alloys). The authors acknowledge useful discussion with G. Benamati, F. Cardellini, F. Cleri (ENEA) and A. Legris (CNRS, University of Lille).

## References

[1] C. Rubbia, J.A. Rubio, S. Buono, F. Carminati, F. Fietier, J. Galvez, C. Geles, Y. Kadi, R. Klapisch, P. Mandrillon, J.P. Revol, Ch. Roche, Conceptual design of a fast neutron operated high power energy amplifier, CERN/AT/95-44(ET), September 1995.
[2] G. Benamati, C. Latge, J.U. Knebel, Technologies for lead alloys, TECLA Project within the Fifth European Framework Program, Ref. No. FIS5-1999-00308, 2000.
[3] M. Salvatores, G.S. Bauer, G. Heusener, The megapie initiative: executive outline and status as per November 1999, MPO-1-GB-6/0-GB.
[4] D. Gomez Briceno, J.F. Martin Munoz, L. Soler Crespo, European Workshop on Heavy Liquid Technology for use in ADS, Foschungzentrum Karlsruhe, September 1999; www.ciemat.es/projectos/pdfntransmutar.html.
[5] V. Rosato, M. Guillope, B. Legrand, Philos. Mag. A 59 (1989) 321.
[6] F. Cleri, V. Rosato, Phys. Rev. B 48 (1993) 22.
[7] B. Joseph, M. Picat, F. Barbier, Eur. Phys. J. AP 5 (1999) 19.
[8] www.webelements.com.
[9] P.N. Martynov, K.D. Ivanov, IAEA Technical Document IAEA-TECDOC 1056, p. 177.
[10] R. Hultgren, P.D. Desai, D.T. Hawkins, M. Gleiser, K.K. Kelley, Selected Values of the Thermodynamic Properties

of Binary Alloys, American Society for Metals, Metals Park, OH, USA, 1973.
[11] W. Gudowski, A. Mellergard, M. Dzugutov, W.S. Howells, P. Zetterstrom, J. Non-Cryst. Solids 156–158 (1993) 130.
[12] R.L. McGreevy, L. Putsztai, Molec. Simul. 1 (1988) 359.
[13] V. Rosato, M. Celino, J. Appl. Phys. 86 (1999) 6826.
[14] M. Asta, D. Morgan, J.J. Hoyt, B. Sadigh, J.D. Althoff, D. de Fontaine, S.M. Foiles, Phys. Rev. B 59 (1999) 14271.
[15] M. Fuchs, M. Scheffler, Comp. Phys. Commun. 119 (1999) 67.